LETTER

doi:10.1038/nature15378

A sexually dimorphic hypothalamic circuit controls maternal care and oxytocin secretion

Niv Scott[1], Matthias Prigge[1], Ofer Yizhar[1] & Tali Kimchi[1]

It is commonly assumed, but has rarely been demonstrated[1,2], that sex differences in behaviour arise from sexual dimorphism in the underlying neural circuits[3,4]. Parental care is a complex stereotypic behaviour towards offspring that is shared by numerous species[5]. Mice display profound sex differences in offspring-directed behaviours. At their first encounter, virgin females behave maternally towards alien pups while males will usually ignore the pups or attack them[6–9]. Here we show that tyrosine hydroxylase (TH)-expressing neurons in the anteroventral periventricular nucleus (AVPV) of the mouse hypothalamus are more numerous in mothers than in virgin females and males, and govern parental behaviours in a sex-specific manner. In females, ablating the AVPV TH$^+$ neurons impairs maternal behaviour whereas optogenetic stimulation or increased TH expression in these cells enhance maternal care. In males, however, this same neuronal cluster has no effect on parental care but rather suppresses intermale aggression. Furthermore, optogenetic activation or increased TH expression in the AVPV TH$^+$ neurons of female mice increases circulating oxytocin, whereas their ablation reduces oxytocin levels. Finally, we show that AVPV TH$^+$ neurons relay a monosynaptic input to oxytocin-expressing neurons in the paraventricular nucleus. Our findings uncover a previously unknown role for this neuronal population in the control of maternal care and oxytocin secretion, and provide evidence for a causal relationship between sexual dimorphism in the adult brain and sex differences in parental behaviour.

The hypothalamus contains several sexually dimorphic nuclei, and has a critical role in coordinating sexual dimorphism in reproductive behaviours and physiological responses to environmental cues[4,10]. Among the sexually dimorphic hypothalamic nuclei, the AVPV (Fig. 1a) is unique as it possesses several female-biased sexually dimorphic characteristics[2,11–13], including a markedly larger number of tyrosine hydroxylase (TH)-immunoreactive neurons in females than in males[4,14]. The presence of TH in these cells suggests that they are dopaminergic, but this has not been tested directly.

We first characterized the TH$^+$ AVPV neurons in adult mice and found that 93% (±1%, $n = 6$ mice) of them co-express DOPA decarboxylase (DDC), the enzyme responsible for the formation of dopamine from DOPA (3,4-dihydroxyphenylalanine) (Fig. 1b). Since dopamine signalling is known to enhance mother–pup interactions[6,15,16], we hypothesized that TH$^+$ AVPV neurons are part of a sexually dimorphic circuit that underlies sex differences in parental care. We first tested whether parenthood is associated with changes in the number of TH$^+$ AVPV cells. In sexually naive (virgin) females, the number of TH-positive neurons was significantly higher than that in virgin males (Fig. 1c, d), consistent with previous work[10,14]. Surprisingly, we further found that in postpartum females this number was significantly higher than in virgin females (725 ± 21 and 493 ± 60, respectively; $P < 0.001$), whereas no such differences were observed between parental and virgin males (271 ± 21 and 273 ± 19, respectively; Fig. 1c, d).

To assess the functional relationship between sexual dimorphism in TH$^+$ AVPV neurons and sex differences in parental behaviour, we employed three complementary cell-type-specific strategies to selectively manipulate TH$^+$ AVPV neurons in adult males and females: selective ablation, overexpression of TH and optogenetic activation (Fig. 2a–e). To ablate TH$^+$ AVPV neurons, we bilaterally injected the neurotoxin 6-hydroxydopamine[17] into the AVPV of wild-type mice. This effectively ablated the majority of TH$^+$ AVPV neurons, but did not affect major TH-expressing neuronal populations in other brain regions (Fig. 2a and Extended Data Fig. 1a–d). Virgin females with bilateral ablation of TH$^+$ AVPV neurons exhibited a profound reduction in maternal displays, including a significantly longer latency to retrieve foreign pups to the nest and a smaller number of pups retrieved compared to control littermates (Fig. 2f, g and Extended Data Fig. 2a, b). TH-ablated virgin females also exhibited a shorter duration of crouching over the pups and a shorter overall duration of maternal behaviour (Fig. 2h and Extended Data Fig. 2c, d). In postpartum females (mothers), TH$^+$ AVPV neuronal ablation induced similar deficits in

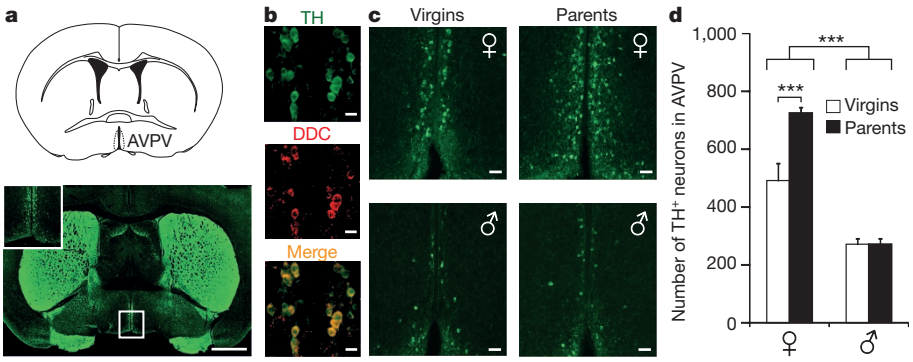

Figure 1 | TH expression in the AVPV is sexually dimorphic and enhanced in postpartum females. **a**, Schematic drawing of mouse AVPV (top) and confocal images of a coronal brain section immunostained for TH (bottom). Inset shows higher magnification image of the AVPV region. Scale bar, 1 mm. **b**, AVPV in a coronal slice from a female mouse immunostained for TH (green) and DDC (red). Scale bars, 20 µm. **c**, Immunostaining for TH in AVPV of female and male virgins and parents. Scale bars, 50 µm. **d**, Total numbers of TH$^+$ neurons in AVPVs of virgin females, virgin males, postpartum females and newly parental males. Data are means ± s.e.m., $n = 5$ per group; ***$P < 0.001$; two-way ANOVA with Fisher's multiple comparisons.

[1]Department of Neurobiology, Weizmann Institute of Science, 76100 Rehovot, Israel.

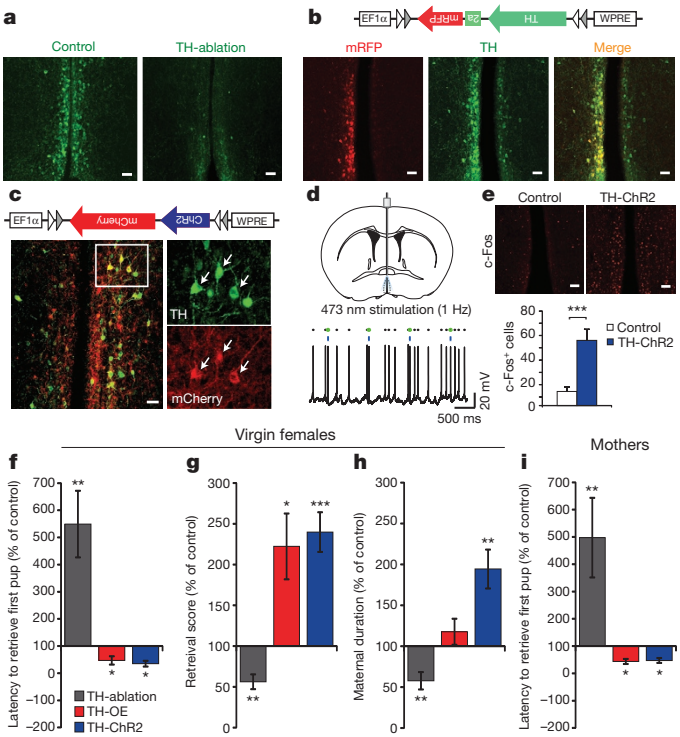

Figure 2 | TH$^+$ AVPV neurons promote maternal behaviour in virgin and postpartum females. **a**, Coronal section of female AVPV immunostained for TH (green). Scale bars, 50 µm. **b**, Schematic drawing of TH overexpression vector (top) and confocal images of coronal sections of unilateral TH-overexpression in the AVPV (bottom). mRFP labels virally transduced neurons (red). TH-immunoreactive neurons are labelled in green. Scale bars, 50 µm. **c**, Schematic drawing of AAV vector used to express ChR2 in TH$^+$ AVPV neurons (top), confocal image depicting ChR2–mCherry expression (red) and TH immunostaining (green) in AVPV neurons (bottom). Scale bar, 50 µm. **d**, Schematic illustration of photostimulation of TH$^+$ AVPV neurons expressing ChR2 (top) and an example voltage recording of a ChR2-expressing AVPV neuron stimulated with light pulses at 1 Hz (bottom). Blue bars represent 10-ms light pulses (475 nm, 19 mW mm^{-2}); black dots indicate detected action potentials; green outlines represent action potentials that are time-locked to light pulses. **e**, Representative images from a TH-ChR2 mouse and TH-EYFP (control) mouse photostimulated in the AVPV. c-Fos-immunoreactive cells are labelled in red (top). Scale bars, 20 µm. Number of c-Fos-expressing cells in AVPV following optogenetic stimulation in TH-ChR2 and control mice (bottom) ($n_{ChR2} = 6$, $n_{control} = 6$, $^{***}P < 0.001$, two-tailed Student's *t*-test). **f**–**h**, Quantification of maternal behaviour of virgin females with TH-ablation (grey bars), TH-OE (red bars) and TH-ChR2 (blue bars) relative to control groups (TH-ablation, $n_{ablation} = 13$, $n_{control} = 13$; TH-OE, $n_{OE} = 9$, $n_{control} = 10$; TH-ChR2, $n_{ChR2} = 12$, $n_{control} = 14$; $^{*}P < 0.05$, $^{**}P < 0.01$, $^{***}P < 0.001$, Mann–Whitney U-test). **i**, Latency to retrieve the 1st pup of postpartum females with TH-ablation, TH-OE and TH-ChR2 relative to control groups (TH-ablation, $n_{ablation} = 11$, $n_{control} = 11$; TH-OE, $n_{OE} = 8$, $n_{control} = 7$; TH-ChR2, $n_{ChR2} = 6$, $n_{control} = 6$; $^{*}P < 0.05$, $^{**}P < 0.01$, Mann–Whitney U-test). Data are means ± s.e.m.

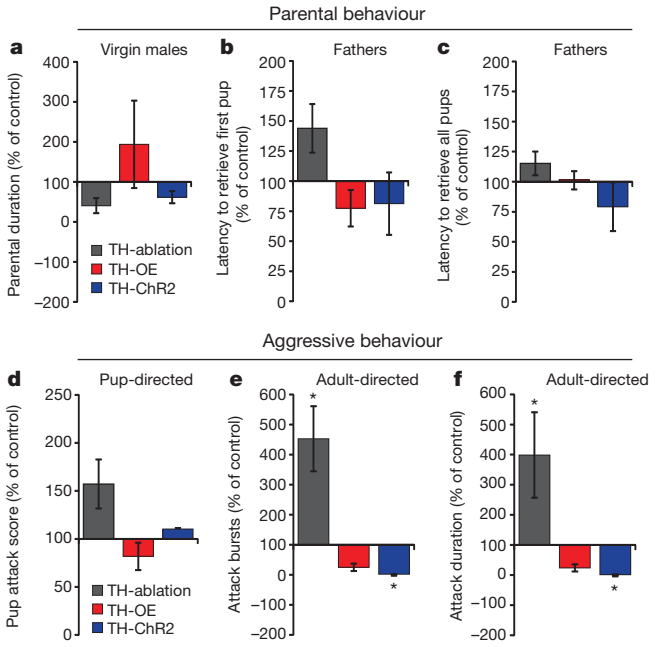

Figure 3 | TH$^+$ AVPV neurons suppress inter-male aggression but do not regulate parental behaviour in males. **a**, **d**, Quantification of pup-directed behaviours of virgin males with TH-ablation, TH-OE and TH-ChR2 relative to control groups. **b**, **c**, Pup retrieval of paternal males with TH-ablation, TH-OE and TH-ChR2 relative to control groups. **e**, **f**, Quantification of inter-male aggression in the resident-intruder test. Data are means ± s.e.m., TH-ablation, $n_{ablation} = 12$, $n_{control} = 12$; TH-OE, $n_{OE} = 10$, $n_{control} = 10$; TH-ChR2, $n_{ChR2} = 8$, $n_{control} = 7$; $^{*}P < 0.05$, Mann–Whitney U-test.

maternal behaviour, manifested as longer latencies to pup retrieval (Fig. 2i and Extended Data Fig. 2e). The AVPV was reported to play a role in the regulation of GnRH neurons (known to control ovulation)[18,19]. However, we found that this TH$^+$-specific ablation in the AVPV did not cause marked changes in female sexual behaviour, oestrous cycle and reproductive success (Extended Data Fig. 3).

The expression level of TH in some dopaminergic neurons is activity-dependent and modulated by sensory stimuli[20,21]. To examine whether elevated TH expression levels in TH$^+$ AVPV neurons are causal in driving maternal behaviour, we overexpressed TH specifically in TH$^+$ AVPV neurons of TH-Cre females using a Cre-dependent TH-expressing adeno-associated virus (AAV) vector (TH-OE; Fig. 2b). In contrast to the effect of TH$^+$ cell ablation, TH-OE promoted maternal behaviour in both virgin and postpartum females (Fig. 2f–i). TH-OE virgin females presented significantly shorter latencies to pup retrieval, and retrieved more pups to the nest compared to virgin females injected with a control mCherry-expressing AAV vector (Fig. 2f, g and Extended Data Fig. 4a, b). Similarly, TH-OE in mothers induced shorter latencies to pup retrieval (Fig. 2i and Extended Data Fig. 4e). This suggests that maternal pup retrieval is facilitated by increased TH levels in TH$^+$ AVPV cells.

To determine whether activation of the TH$^+$ AVPV circuit can promote maternal behaviour, we injected virgin TH-Cre females with a Cre-dependent channelrhodopsin-2 AAV vector into the AVPV (TH-ChR2; Fig. 2c). We first recorded in acute brain slices from ChR2$^+$ and ChR2$^-$ neurons in the AVPV to verify effective photostimulation of ChR2-expressing cells. The spontaneous firing rates of TH$^+$ AVPV neurons were similar to those described previously for AVPV neurons[22], and their intrinsic electrophysiological properties resembled those of midbrain dopaminergic neurons[23] (Fig. 2d and Extended Data Fig. 5a–j). We also confirmed *in vivo* activation of these neurons using c-Fos staining (Fig. 2e). Tonic 1 Hz photostimulation of TH$^+$ AVPV neurons in virgin females elicited a shorter latency to retrieve pups to the nest and increased the number of pups retrieved (Fig. 2f, g; Extended Data Fig. 6a, b and Supplementary Videos 1, 2). Moreover, photostimulation promoted crouching behaviour and prolonged the overall duration of maternal care (Fig. 2h and Extended Data Fig. 6c, d). Similarly, activation of TH$^+$ AVPV neurons in mothers promoted pup retrieval to the nest, but did not affect maternal aggression, an adult-directed aggressive behaviour in lactating dams (Fig. 2i and Extended Data Fig. 6e–g). In all of the TH-manipulated groups, we verified that the observed effects on maternal behaviour are not accompanied by changes in anxiety, exploration, or locomotor activity (Extended Data Fig. 7a–l). These findings indicate that TH$^+$ AVPV neurons are required for the control of maternal behaviour in virgin and postpartum females.

We next examined whether TH$^+$ AVPV neurons are involved in the regulation of parental behaviour in males. To address this, we manipulated TH$^+$ AVPV neurons in males using the same TH-specific strategies. In contrast to the robust effects seen in females, neither ablation nor TH-overexpression or optogenetic activation of TH$^+$ AVPV neurons induced significant changes in parental behaviour in virgin and parental (fathers) males (Fig. 3a–c, Extended Data Figs 2f–h, 4f–h and 6h–j). Notably, however, ablation of TH$^+$ AVPV neurons in virgin males induced a trend towards increased pup-directed aggression ($P = 0.09$; Fig. 3d and Extended Data Fig. 2h). To further assess whether TH$^+$ AVPV cells contribute to the regulation of male aggression, we tested the effects of our TH-manipulations on inter-male aggression by using the resident–intruder assay[24]. We found that males in which TH$^+$ AVPV neurons were ablated presented an increase in attack bursts and in the total duration of aggression (Fig. 3e, f and Extended Data Fig. 2i, j). In contrast, optogenetic activation of TH$^+$ AVPV neurons led to a significant reduction in these behavioural measures (Fig. 3e, f; Extended Data Fig. 6k, l and Supplementary Videos 3, 4). TH-manipulated males displayed no changes in anxiety, exploration or locomotor activity (Extended Data Fig. 8a–j). We conclude that in males, TH$^+$ AVPV neurons act as negative regulators of inter-male aggression but do not contribute to regulation of parental care.

Several hormones, including oestradiol, corticosterone, prolactin and oxytocin, have been implicated in the regulation of sex-specific parental behaviour[16,25]. This could suggest that the regulation of maternal behaviour by TH$^+$ AVPV neurons is associated with the action of these hormones. We measured changes in the peripheral levels of these hormones in the absence of pups (Fig. 4a and Extended Data Fig. 9a–e). We found that oxytocin (OT) levels, but not the levels of other hormones, were reduced following TH$^+$ AVPV neuronal ablation and elevated in TH-OE virgin females compared to controls (Fig. 4a and Extended Data Fig. 9b, d, e). Remarkably, we further found that optogenetic stimulation of TH$^+$ AVPV neurons at 1 Hz for 10 min was sufficient to induce a significant increase in OT levels in ChR2-expressing virgin females (Fig. 4a). In contrast, none of the TH$^+$ AVPV manipulations induced significant changes in circulating OT levels in virgin males (Extended Data Fig. 9a). TH$^+$ AVPV neurons thus seem to directly regulate the release of circulating OT in females.

We next explored the anatomical and functional connectivity between TH$^+$ AVPV neurons and OT-secreting neurons in the paraventricular nucleus (PVN) and the supraoptic nucleus (SON)[26]. We fluorescently labelled the axonal projections of the TH$^+$ AVPV neurons by injecting a Cre-dependent enhanced yellow fluorescent protein (EYFP)-expressing viral vector into the AVPV of TH-Cre mice. Projection analysis revealed several brain regions containing fluorescently labelled TH$^+$ fibres in both males and females (Extended Data Fig. 10a–d). Among the brain regions that showed the densest projections were the medial preoptic area, a region associated with parental behaviour[6,27,28], and the PVN. Immunostaining for OT in the PVN revealed dense TH$^+$ AVPV fibres in close proximity to OT$^+$ PVN neurons (Fig. 4b). Additionally, we injected a Cre-dependent anterograde viral tracer (H129ΔTK-TT) into the AVPV of TH-Cre females. Immunohistochemical staining for OT in the PVN showed that 55 ± 7% of OT$^+$ neurons co-labelled with the anterograde virus (Fig. 4c, e). In contrast, similar staining in the SON did not reveal any virally-transduced OT$^+$ neurons (Fig. 4d, e).

To test for a functional synaptic connection between TH$^+$ AVPV neurons and OT$^+$ PVN cells, we obtained whole-cell patch clamp recordings from PVN OT$^+$ cells and photostimulated ChR2$^+$ axonal projections from the AVPV. For these recordings, we labelled OT$^+$ PVN neurons of TH-Cre females with an AAV vector encoding the Venus fluorophore under an OT promoter. A second AAV, encoding a Cre-dependent ChR2–mCherry fusion protein, was injected into the AVPV. Acute slices prepared from these mice showed ChR2–mCherry-labelled fibres throughout the region containing

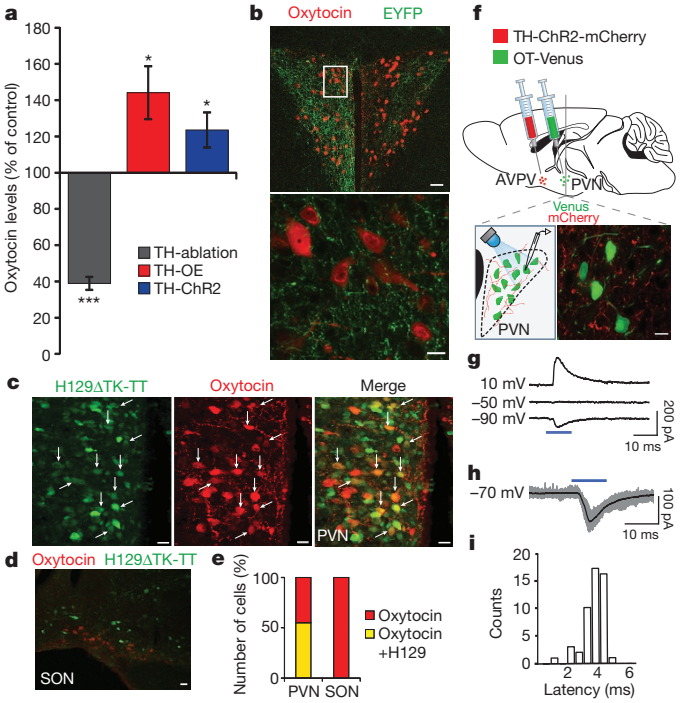

Figure 4 | TH$^+$ AVPV neurons form synaptic connections with OT$^+$ PVN neurons and regulate OT secretion in females. **a**, Plasma OT levels in TH-ablation, TH-OE and TH-ChR2 females relative to control groups (data are means ± s.e.m., TH-ablation, $n_{ablation} = 8$, $n_{control} = 5$; TH-OE, $n_{OE} = 9$, $n_{control} = 9$; TH-ChR2, $n_{ChR2} = 7$, $n_{control} = 8$; $^*P < 0.05$, $^{***}P < 0.001$, two-tailed Student's *t*-test). **b**, Coronal sections of the PVN in TH-Cre female injected unilaterally with Cre-dependent EYFP vector into the AVPV. Anterograde fibres projecting from TH$^+$ AVPV neurons (green) lie in the vicinity of OT$^+$ neurons in the PVN (red). Scale bars, 50 µm (top) and 10 µm (bottom). **c**, Coronal sections of TH-Cre female injected with Cre-dependent anterograde tracer (H129ΔTK-TT) into the AVPV, showing virally labelled OT$^+$ neurons in the PVN. Arrows indicate virally transduced neurons (green pseudocolour) that are OT$^+$ (red pseudocolour). Scale bars, 10 µm. **d**, Coronal section of the SON of TH-Cre female injected with Cre-dependent anterograde tracer into the AVPV, showing virally labelled neurons (green) and OT$^+$ neurons (red). Scale bar, 10 µm. **e**, Percentage of virally transduced OT$^+$ neurons in the PVN and SON (PVN: 55 ± 7%, SON: none, $n = 3$ mice). **f**, Illustration of the experimental approach. Top, schematic drawing of a mouse brain in a sagittal view injected with AAV-DIO-ChR2-mCherry into the AVPV and with AAV-OT-Venus into the PVN. Bottom, schematic drawing and confocal image of PVN coronal section showing the OT$^+$ neurons transduced with AAV-OT-Venus (green) and fibres from TH$^+$ AVPV neurons expressing ChR2–mCherry (red). Scale bar, 10 µm. **g**, Light-evoked responses in OT$^+$ cells recorded in voltage clamp mode at the specified holding potentials. **h**, Average light response (black) overlays 50 single-trial responses (grey) of a representative OT$^+$ cell clamped to −70 mV. **i**, Distribution of light-induced response latencies from 50 light stimuli recorded in a single OT$^+$ cell (median = 3.77 ms from light onset). SON, supraoptic nucleus; PVN, paraventricular nucleus.

OT$^+$ neurons, confirming the results of our viral tracing experiments (Fig. 4f). Photostimulation of TH-ChR2 fibres in the PVN evoked fast excitatory post-synaptic currents in 7 out of 19 OT$^+$ PVN neurons recorded (3.81 ± 0.83 ms latency from blue light onset; $n = 7$ cells from 3 mice; Fig. 4g–i). These results indicate that a monosynaptic connection exists between the TH$^+$ AVPV neurons and OT$^+$ PVN cells, suggesting that TH$^+$ AVPV neurons can facilitate OT release from OT$^+$ PVN neurons.

Our study reveals that a female-biased cluster of TH-expressing neurons in the AVPV has an essential role in the control of sex-specific behaviours in both sexes. Whereas in females this neural population acts to promote maternal care and OT secretion, in males it is rather involved in the suppression of adult-directed aggression. Moreover, we

have uncovered a novel monosynaptic circuit linking the TH^+ AVPV neurons with PVN OT^+ neurons. In rodents, as in many mammals, OT signalling is necessary for lactation and has been implicated as a central neuroendocrine mediator of maternal behaviour[5,25,29,30]. Based on our findings and on these previous reports, we propose that in females, pup-mediated signals trigger the activation of TH^+ AVPV neurons, which in turn activate oxytocinergic neurons in the PVN, releasing OT into the brain and periphery and facilitating instinctive parental behaviours (Extended Data Fig. 10e).

Finally, although manipulation of TH^+ AVPV neurons markedly altered sex-specific behaviours in both males and females, the behaviours displayed by manipulated animals of both sexes did not exceed the boundaries of sex-typical behaviours. These data highlight the critical role of intrinsic sex differences in the brain in setting the distinct behavioural repertoire displayed by males and females. Within these boundaries, changes in the activity of sexually-dimorphic neural circuits allow dynamic modulation of adaptive behavioural responses to sex-specific challenges.

Online Content Methods, along with any additional Extended Data display items and Source Data, are available in the online version of the paper; references unique to these sections appear only in the online paper.

Received 22 March; accepted 31 July 2015.
Published online 16 September 2015.

1. Xu, X. *et al.* Modular genetic control of sexually dimorphic behaviors. *Cell* **148,** 596–607 (2012).
2. Yang, C. F. *et al.* Sexually dimorphic neurons in the ventromedial hypothalamus govern mating in both sexes and aggression in males. *Cell* **153,** 896–909 (2013).
3. De Vries, G. J. & Villalba, C. Brain sexual dimorphism and sex differences in parental and other social behaviors. *Ann. NY Acad. Sci.* **807,** 273–286 (1997).
4. Simerly, R. B. Wired for reproduction: organization and development of sexually dimorphic circuits in the mammalian forebrain. *Annu. Rev. Neurosci.* **25,** 507–536 (2002).
5. Dulac, C., O'Connell, L. A. & Wu, Z. Neural control of maternal and paternal behaviors. *Science* **345,** 765–770 (2014).
6. Kuroda, K. O., Tachikawa, K., Yoshida, S., Tsuneoka, Y. & Numan, M. Neuromolecular basis of parental behavior in laboratory mice and rats: with special emphasis on technical issues of using mouse genetics. *Prog. Neuropsychopharmacol. Biol. Psychiatry* **35,** 1205–1231 (2011).
7. Vom Saal, F. S. Time-contingent change in infanticide and parental behavior induced by ejaculation in male mice. *Physiol. Behav.* **34,** 7–15 (1985).
8. Chalfin, L. *et al.* Mapping ecologically relevant social behaviours by gene knockout in wild mice. *Nat. Commun.* **5,** 4569 (2014).
9. Lonstein, J. S. & De Vries, G. J. Sex differences in the parental behavior of rodents. *Neurosci. Biobehav. Rev.* **24,** 669–686 (2000).
10. Semaan, S. J. & Kauffman, A. S. Sexual differentiation and development of forebrain reproductive circuits. *Curr. Opin. Neurobiol.* **20,** 424–431 (2010).
11. Simerly, R. B. Organization and regulation of sexually dimorphic neuroendocrine pathways. *Behav. Brain Res.* **92,** 195–203 (1998).
12. Cao, J. & Patisaul, H. B. Sexually dimorphic expression of hypothalamic estrogen receptors α and β and Kiss1 in neonatal male and female rats. *J. Comp. Neurol.* **519,** 2954–2977 (2011).
13. Zuloaga, D. G., Zuloaga, K. L., Hinds, L. R., Carbone, D. L. & Handa, R. J. Estrogen receptor β expression in the mouse forebrain: age and sex differences. *J. Comp. Neurol.* **522,** 358–371 (2014).
14. Simerly, R. B., Zee, M. C., Pendleton, J. W., Lubahn, D. B. & Korach, K. S. Estrogen receptor-dependent sexual differentiation of dopaminergic neurons in the preoptic region of the mouse. *Proc. Natl Acad. Sci. USA* **94,** 14077–14082 (1997).
15. Love, T. M. Oxytocin, motivation and the role of dopamine. *Pharmacol. Biochem. Behav.* **119,** 49–60 (2014).
16. Lonstein, J. S. & Morrell, J. I. in *Handbook of Neurochemistry and Molecular Neurobiology: Behavioral Neurochemistry, Neuroendocrinology and Molecular Neurobiology* (eds Lejtha, A. & Blaustein J.) Ch. 5, 197–229 (Springer-Verlag, 2007).
17. Iancu, R., Mohapel, P., Brundin, P. & Paul, G. Behavioral characterization of a unilateral 6-OHDA-lesion model of Parkinson's disease in mice. *Behav. Brain Res.* **162,** 1–10 (2005).
18. Liu, X. & Herbison, A. E. Dopamine regulation of gonadotropin-releasing hormone neuron excitability in male and female mice. *Endocrinology* **154,** 340–350 (2013).
19. Han, S. K. *et al.* Activation of gonadotropin-releasing hormone neurons by kisspeptin as a neuroendocrine switch for the onset of puberty. *J. Neurosci.* **25,** 11349–11356 (2005).
20. Spitzer, N. C. Activity-dependent neurotransmitter respecification. *Nature Rev. Neurosci.* **13,** 94–106 (2012).
21. Aumann, T. D., Tomas, D. & Horne, M. K. Environmental and behavioral modulation of the number of substantia nigra dopamine neurons in adult mice. *Brain Behav.* **3,** 617–625 (2013).
22. Ducret, E., Gaidamaka, G. & Herbison, A. E. Electrical and morphological characteristics of anteroventral periventricular nucleus kisspeptin and other neurons in the female mouse. *Endocrinology* **151,** 2223–2232 (2010).
23. Margolis, E. B., Lock, H., Hjelmstad, G. O. & Fields, H. L. The ventral tegmental area revisited: is there an electrophysiological marker for dopaminergic neurons? *J. Physiol. (Lond.)* **577,** 907–924 (2006).
24. Kimchi, T., Xu, J. & Dulac, C. A functional circuit underlying male sexual behaviour in the female mouse brain. *Nature* **448,** 1009–1014 (2007).
25. Rilling, J. K. & Young, L. J. The biology of mammalian parenting and its effect on offspring social development. *Science* **345,** 771–776 (2014).
26. Lee, H.-J., Macbeth, A. H., Pagani, J. H. & Young, W. S. III. Oxytocin: the great facilitator of life. *Prog. Neurobiol.* **88,** 127–151 (2009).
27. Wu, Z., Autry, A. E., Bergan, J. F., Watabe-Uchida, M. & Dulac, C. G. Galanin neurons in the medial preoptic area govern parental behaviour. *Nature* **509,** 325–330 (2014).
28. Numan, M. & Woodside, B. Maternity: neural mechanisms, motivational processes, and physiological adaptations. *Behav. Neurosci.* **124,** 715–741 (2010).
29. Numan, M. & Insel, T. R. *The Neurobiology of Parental Behavior* (Springer-Verlag, 2003).
30. Marlin, B. J., Mitre, M., D'amour, J. A., Chao, M. V. & Froemke, R. C. Oxytocin enables maternal behaviour by balancing cortical inhibition. *Nature* **520,** 499–504 (2015).

Supplementary Information is available in the online version of the paper.

Acknowledgements We thank M. Dayan, E. Elharrar, I. Sofer, Y. Pen, Y. Beny, N. Zhilka and E. Massasa for their assistance with the experiments; R. Levy for help with virus production; A. Chen and A. Ramot for sharing equipment and reagents. A. Mizrahi, S. Wagner, and the Yizhar and Kimchi groups, for comments on the manuscript; D. Anderson for providing the Cre-dependent anterograde virus and V. Grinevich for providing the OT:Venus virus. M.P. was supported by the Clore Center for Biological Physics and a Minerva postdoctoral fellowship. This work was supported by grants from Minerva Foundation 711131, Women's Health Research Center, Gruber Foundation 720667, ISF 1324/15, the Jenna and Julia Birnbach Career Development Chair to T.K.; and Marie Curie CIG 321919, ERC StG 337637, ISF 1351/12, the Nollman Career Development Chair to O.Y.

Author Contributions N.S. performed all behavioural, neuronal tracing and *in vivo* physiological experiments. M.P. cloned the TH-overexpression viral vector and performed the *in vitro* electrophysiology experiments. O.Y. supervised the electrophysiology experiments and assisted in designing the optogenetic assays. T.K. planned and supervised all the experiments. T.K. and N.S. interpreted the results and wrote the paper together with M.P. and O.Y.

Author Information Reprints and permissions information is available at www.nature.com/reprints. The authors declare no competing financial interests. Readers are welcome to comment on the online version of the paper. Correspondence and requests for materials should be addressed to T.K. (tali.kimchi@weizmann.ac.il) or O.Y. (ofer.yizhar@weizmann.ac.il)

METHODS

Animals. Male and female mice (12 to 20 weeks old) were used in all experiments. For TH-ablation experiments wild-type mice (CD-1-Harlan Laboratory) were used. For TH-overexpression, TH^+ optogenetic stimulation and tracing experiments, TH-IRES-Cre[31] male and female mice were used. Littermates were randomly assigned to experiment or control groups. We confirmed the specificity of Cre-expressing neurons in virgin females by showing that a majority of Cre-expressing cells overlap with TH-immunoreactive cells in the AVPV (EYFP (Cre) cells expressing TH = 80 ± 3%; TH cells expressing EYFP (Cre) = 91 ± 3%, $n = 6$ mice). Compared with reports of reduced specificity of this mouse line to dopamine neurons in the ventral tegmental area[32], these data indicate that specificity in the AVPV is relatively high. Furthermore, increased TH expression in maternal females might further increase the specificity values. All mice were bred and housed in a specific-pathogen-free animal facility; they were maintained on a reverse 12:12 h light–dark cycle with food and water *ad libitum*. All experimental procedures were approved by the Institutional Animal Care and Use Committee (IACUC) at the Weizmann Institute of Science.

Viral vectors. pAAV5-Ef1α-DIO-ChR2(E123T/T159C)-mCherry, pAAV5-EF1α-DIO-EYFP and pAAV5-Ef1α-DIO-mCherry were acquired from UNC Gene Therapy Center. H129-ΔTK-TT virus[33] was a gift of D. J. Anderson and AAV-OTpr-Venus virus[34] was a gift of V. Grinevich. A Cre-dependent vector for TH-overexpression (pAAV-EF1α-DIO-TH-p2A-mRFP) was produced using overlap extension PCR. A 2A peptide was inserted between TH and mRFP coding sequences to allow unperturbed function of TH. The forward and reverse primer for the entire PCR fragment contained an AscI and NheI restriction sites. The resulting amplicon was digested and cloned into the pAAV-EF1α-DIO backbone[35].

6-OHDA. 6-hydroxydopamine hydrochloride (Sigma-Aldrich) was dissolved in 0.1% ascorbic acid saline solution to final concentration of 6 μg μl^{-1} and prepared fresh every day before injections into the AVPV.

Surgery. Mice were anaesthetized with isoflurane and mounted on a stereotaxic frame (myNeuroLab). Virus or agent was bilaterally or unilaterally injected into the AVPV (for behaviour or tracing, respectively) using a Hamilton syringe at an injection rate of 0.05–0.15 μl min^{-1}. AVPV injection coordinates were anteroposterior (AP): 0.25 mm, mediolateral (ML): ±0.15 mm, dorsoventral (DV): −5.45 mm. Injection volumes were: 0.2 μl for TH-OE and ChR2 viruses; 0.06 μl and 0.1 μl for AAV-EYFP and H129ΔTK-TT tracing experiments, respectively; 1 μl for 6-OHDA. AAV-OTpr-Venus was bilaterally injected into the PVN (AP: −0.8 mm, ML: ±0.2, DV: −4.75) at a volume of 0.3 μl. ChR2 animals used for behavioural testing were implanted with 200 μm fibre-optic cannulae (Thorlabs). Fibres were located medially and above the AVPV of both hemispheres (Fig. 2d). The cannula was secured using dental cement. Mice were left to recover for at least 3 weeks before behavioural assays.

Behavioural assays. All behavioural tests were performed during the dark phase and under dim red light. Behaviours were recorded using a digital video recording unit and scored using Observer XT or EthoVision softwares (Noldus Information Technology) by an individual blind to the identity of the manipulated groups.

Parental behaviour. Males and females were tested for pup-directed behaviours using the exact same behavioural assay procedure. Mice were individually housed with nesting material (cotton) 24 h before the trial. Three newborn alien pups (1–3 days old, CD-1, Harlan Laboratories) were placed on the opposite side to the sleeping nest in the resident mouse's home cage and behaviour was recorded for 15 min. Females were introduced to pups for 3 consecutive days and parental behaviours were scored on day 3 when animals exhibited the highest level of parental behaviour. Pup-directed behaviours of males were scored on day 1 since their behaviour did not change with repeated exposure to pups. The scored behavioural parameters were (Supplementary Videos 1, 2): pup retrieval, carrying the pups to the cotton nest; crouching, covering the pups to maintain body temperature and (in females) lactating behaviour; nesting, building a nest around the pups; licking, licking the pups; attack, pup-directed attack; ignore, failing to approach or make contact with the pups. Parental duration was taken as the sum of all parental behaviour durations in the assay: crouching, nesting and licking. Pup retrieval was scored in points and quantified as a cumulative retrieval score in which each successful pup retrieval to the nest contributed 1 point. Pup-directed aggression (attack score) was quantified similarly, with each pup attack contributing 1 point. Parental behaviours in postpartum females were tested on postpartum day 4. For this assay, first all newborn pups were removed from the home cage of each female mouse, and then after 10 min, three of the female's own pups were placed back in the resident's home cage on the opposite side to the breeding nest for 10 min. Latencies to retrieval of the pups back to the nest were scored as described above. Fathers' parental behaviour was measured in males that were housed together with females for 21–24 days (that is, separated from the lactating females and their own pups 1–3 days after the delivery of the pups).

Maternal aggression. Postpartum females were tested for maternal aggression 8 days post-delivery. All pups were removed from cage and adult intruder male was immediately introduced to female cage for 10 min assay. Females were scored for the duration and number of their aggressive attacks towards the intruder male.

Female sexual behaviour. For 4 consecutive days oestrus cycle state was determined (see below). Only females confirmed to be in oestrus were introduced with an experienced male for 15 min assay. Female receptivity was scored as lordosis, successful male mountings and male rejections.

Male–male interactions. Males were separated to their home cages and introduced to 6 to 7 week-old C57Bl/6 unfamiliar male intruders for 10 min. The male intruders were swabbed with 60 μl urine collected from sexually mature and experienced male mice. All experiments were videotaped and the behaviours of the resident animals were scored for the following parameters: number of attacks, latency to attack and total duration of aggression (Supplementary Videos 3, 4).

Open-field assay. The test was performed in a white Plexiglas box (50 × 50 × 40 cm) with an overhead lamp directed to the centre of the field, providing 120 lx of illumination on the floor. Each mouse was placed in the corner of the apparatus and its locomotion pattern was recorded for 10 min.

Elevated plus maze assay. The test was performed using a polyvinyl chloride maze comprising a central part (5 × 5 cm), two opposing open arms (30.5 × 5 cm), and two opposing closed arms (30.5 × 5 × 15 cm). The apparatus was raised to a height of 53.5 cm, and the open arms were provided with 6 lx of illumination. Each mouse was placed in the centre facing an open arm and its locomotion was recorded for 5 min. The distance travelled and time spent in the open arms was measured.

ChR2 mediated *in vivo* photostimulation. Prior to all behavioural tests, animals were connected to optical fibres with a 200-μm silica core (BFL37-200; Thorlabs) for 5–10 min habituation. To enable free movement during the test, we connected the optical fibres to an optical rotary joint (Doric Lenses QC, Canada). Light stimulation at 473 nm was provided by a DPSS laser (CrystaLaser) and lasted for the entire duration of the assay. Photostimulation of TH^+ AVPV neurons was most effective at low frequencies (<10 Hz) and its efficacy declined at higher frequencies (Extended Data Fig. 5b). Photostimulation parameters in all assays were 1 Hz frequency, 10 ms pulse-width and 95 mW mm^{-2} light power density. Laser pulses were driven by a 33220A Function Waveform Generator (Agilent Technologies, Israel). For c-Fos verification, mice were stimulated with a train of 473 nm light (5 Hz, 10 ms) for 30 min. Mice were euthanized 60 min post-stimulation and brains were processed for immunohistochemistry. The activation frequency of 5 Hz was chosen as we observed efficient excitation of the neurons using this frequency in the acute slice preparation.

Slice electrophysiology recording. Four to eight weeks after virus injection, 300-μm-thick coronal sections of the AVPV and PVN were prepared using a vibratome (Leica TV1200S) in ice-cold sucrose cutting solution (in mM: 11 D-glucose, 234 sucrose, 2.5 KCl, 1.25 NaH_2PO_4, 10 $MgSO_4$, 0.5 $CaCl_2$, 26 $NaHCO_3$) oxygenated with 95% O_2/5% CO_2. Slices were then incubated at 32 °C for 30 min in high-osmolarity artificial cerebrospinal fluid (aCSF; in mM: 3.24 KCl, 11.88 glucose, 132.8 NaCl, 28.1 $NaHCO_3$, 1.35 NaH_2PO_4, 1.08 $MgCl_2$, 2.16 $CaCl_2$; 320 mOsm kg^{-1}, aerated with 95% O_2/5% CO_2) and another 30 min in iso-osmotic aCSF (in mM: 3 KCl, 11 glucose, 123 NaCl, 26 $NaHCO_3$, 1.25 NaH_2PO_4, 1 $MgCl_2$, 2 $CaCl_2$; 300 mOsm kg^{-1}, aerated with 95% O_2/5% CO_2) at 32 °C. Following recovery, slices were kept at room temperature until use. The recording chamber was perfused with oxygenated aCSF at a rate of 1.5-2 ml min^{-1} and maintained at 32 °C. Borosilicate glass pipettes (Sutter Instrument BF100-58-10) with resistances ranging from 4–6 MΩ were pulled using a laser micropipette puller (Sutter Instrument Model P-2000) and filled with intracellular solution (in mM: 135 K-gluconate, 4 KCl, 2 NaCl, 10 HEPES, 4 EGTA, 4 MgATP, 0.3 NaTRIS, 280 mOsm kg^{-1}, pH adjusted to 7.3 with KOH). Recordings in PVN OT cells were performed with an intracellular solution (in mM: 120 CS-gluconate, 11 CsCl, 1 $MgCl_2$, 1 $CaCl_2$, 10 HEPES, 11 EGTA, 5 QX-314, 280 mOsm kg^{-1}, pH adjusted to 7.3 with CsOH). Neurons were patched under visual guidance using infrared differential interference contrast (DIC) microscopy (Olympus BX51WIF) and an Andor Clara CCD camera. OT cells were identified based on Venus fluorescence. Recordings were carried out using a Multiclamp 700B amplifier (Axon Instruments). Optical activation of ChR2-expressing neurons was performed using 475/28 nm and 10 ms light pulses at 19 mW mm^{-2} (Lumencor Spectra-X) delivered through the microscope illumination path.

Oestrus cycle analysis. Oestrous cycle stage of females was determined for 9 consecutive days. Each day at 10am a vaginal smear was collected from all females, stained with Dip Quick stain kit (Jorgensen Laboratories, Inc.) and analysed for oestrus under a light microscope. The stage of the oestrus cycle was determined as previously described[36].

Hormone level analysis. Upon completion of behavioural assays, mice were anaesthetized with isoflurane and blood samples were collected from the orbital

sinus. The blood was centrifuged and the supernatant was collected and stored at −80 °C. Plasma oxytocin, corticosterone, oestradiol and prolactin levels were measured using ELISA kits according to the manufacturers' protocols (Enzo Life Sciences - ADI-900-153 for oxytocin, Cayman Chemical Company - 500655 for corticosterone and 582251 for oestradiol, abcam - ab100736 for prolactin).

Immunohistochemistry. Following behavioural assays and blood collection the mice were euthanized, perfused with 4% paraformaldehyde (PFA), and their brains were sectioned with a vibratome (Leica Microsystems) into 30–50 µm coronal slices. Floating brain slices were collected, washed three times in PBS, and immunostained for tyrosine hydroxylase (TH), DOPA decarboxylase (DDC), GFP, oxytocin (OT) or c-Fos using the following protocol. For 24–48 h at 4 °C, slices were incubated in blocking solution: 10% to 20% normal human serum (NHS), 0.04% Triton; carrier: 1% NHS, 0.03% Triton; primary antibodies: rabbit/sheep anti-TH (1:1,000, Millipore), rabbit anti-DDC (1:1,000, Novus), goat anti-GFP biotinylated (1:200-1,000, Abcam), rabbit anti-c-Fos (1:1,000, Santa Cruz) and guinea-pig/rabbit anti-OT (1:1,000, Peninsula Laboratories LLC) for 24−48 h at 4 °C; secondary antibodies: Cy3-goat anti-rabbit, Cy5-donkey anti-guinea pig (1:200, Jackson ImmunoResearch), Alexa Flour 488-conjugated streptavidin, Alexa Flour 488/594 anti-rabbit, Alexa Flour 488/594 anti-sheep (1:200, Molecular Probes).

Image analysis and cell counting. All brain slices were imaged by epifluorescence microscopy (Nikon, Eclipse 80i) or by confocal microscopy (Zeiss, LSM 710) for subsequent analysis. Brain areas were determined according to their anatomy using Franklin and Paxinos Brain Atlas. For AVPV TH^+ cell counts the entire AVPV was sliced, stained and counted. For c-Fos, anterograde tracing, viral infection and 6-OHDA lesion specificity experiments, cell counts were performed on selected brain slices, chosen in each animal according to standard anatomical markers. All counts were done manually by experimenter blind to test conditions.

Anterograde tracing. Mice injected unilaterally with AAV-DIO-EYFP virus were perfused 5 weeks post-injection, and their brains were sectioned coronally (50 µm slices) and mounted on slides. Each brain area in which EYFP-immunoreactive fibres were detected was scanned by confocal microscope under uniform imaging settings (LSM 710, Zeiss, Germany). Representative brain images were analysed for projection intensity using ImageJ software. For trans-synaptic anterograde tracing, females injected unilaterally with H129ΔTK-TT were perfused 5 to 7 days post-injection as previously described[28]. The brains were sectioned into 50 µm coronal slices, and these were mounted on slides and analysed to verify the injection site. Brain slices from the PVN and the SON were immunostained with anti-oxytocin antibody and imaged by confocal microscopy for further analysis of colocalization with dtTomato-labelled virally transduced neurons.

Statistical analysis. Sample size was determined according to the accepted practice for behavioural assays, but no statistical methods were used to predetermine sample size. All data are expressed as means ± s.e.m. Behavioural assays were analysed using the non-parametric Mann–Whitney U-tests. Two-way ANOVA with post-hoc tests or two-tailed student's *t*-tests were used for statistical evaluation of immunostaining assays, tracing experiments and hormone analyses. Outlier samples (more than 2S.D. from the mean in >2 parameters) were excluded from experiment. All statistical tests were performed using STATISTICA software (StatSoft, Tulsa, OK).

31. Lindeberg, J. *et al.* Transgenic expression of Cre recombinase from the tyrosine hydroxylase locus. *Genesis* **40,** 67–73 (2004).
32. Lammel, S. *et al.* Diversity of transgenic mouse models for selective targeting of midbrain dopamine neurons. *Neuron* **85,** 429–438 (2015).
33. Lo, L. & Anderson, D. J. A Cre-dependent, anterograde transsynaptic viral tracer for mapping output pathways of genetically marked neurons. *Neuron* **72,** 938–950 (2011).
34. Knobloch, H. S. *et al.* Evoked axonal oxytocin release in the central amygdala attenuates fear response. *Neuron* **73,** 553–566 (2012).
35. Sohal, V. S., Zhang, F., Yizhar, O. & Deisseroth, K. Parvalbumin neurons and gamma rhythms enhance cortical circuit performance. *Nature* **459,** 698–702 (2009).
36. Nelson, J. F., Felicio, L. S., Randall, P. K., Sims, C. & Finch, C. E. A longitudinal study of estrous cyclicity in aging C57BL/6J mice: I. Cycle frequency, length and vaginal cytology. *Biol. Reprod.* **27,** 327–339 (1982).

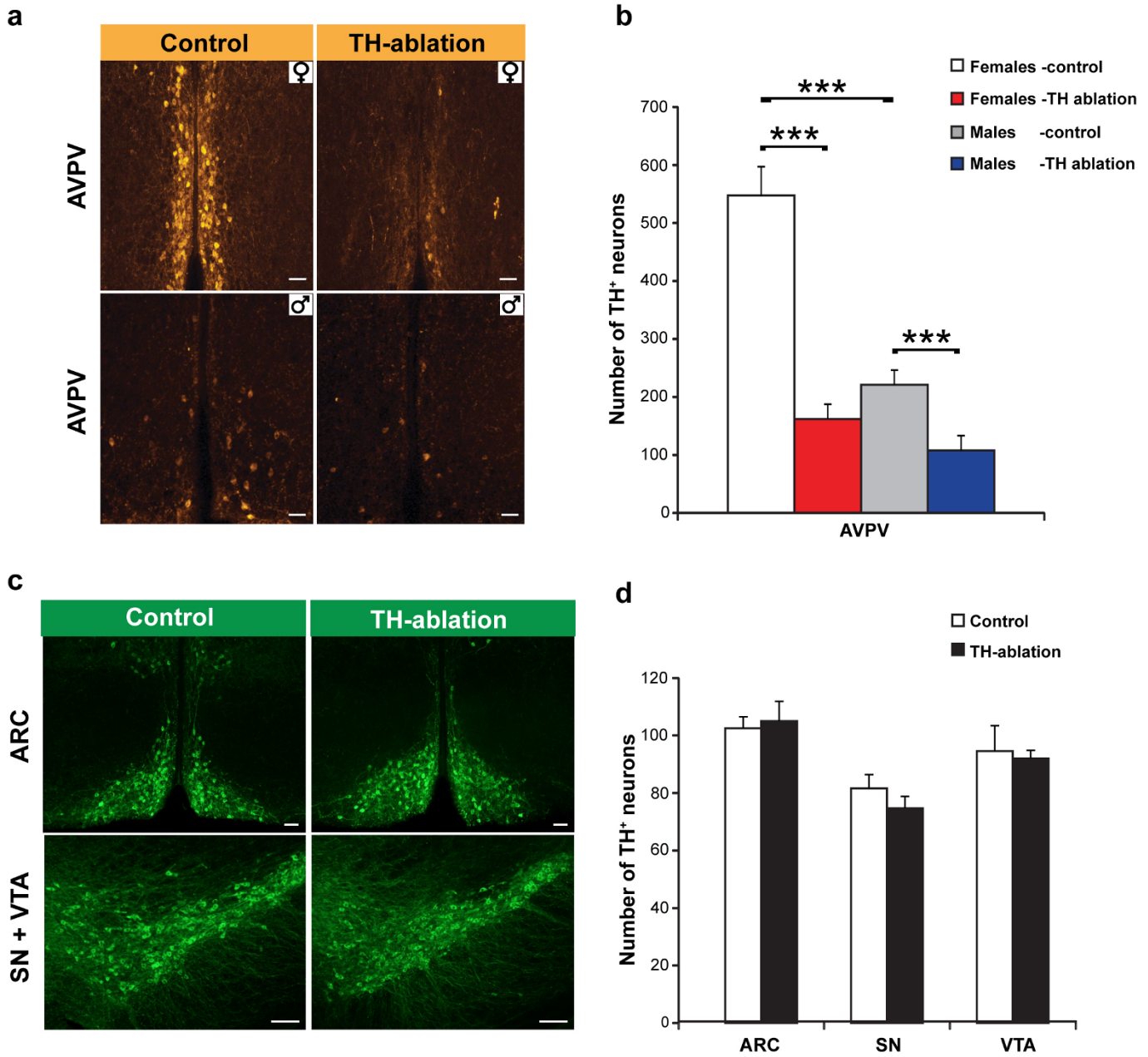

Extended Data Figure 1 | 6-OHDA injection into AVPV of male and female mice results in specific ablation of TH$^+$ neurons. **a**, TH immunostaining in AVPVs of females and males injected with 6-OHDA (TH-ablation) or saline (control). Scale bars, 20 µm. **b**, Number of TH$^+$ AVPV neurons in TH-ablation and control females and males (females, $n_{\text{TH-ablation}} = 12$, $n_{\text{control}} = 13$; males, $n_{\text{ablation}} = 9$, $n_{\text{control}} = 8$; $^{***}P < 0.001$, two-way ANOVA with Fisher's multiple comparisons). **c**, TH immunostaining in brain slices from females injected with 6-OHDA or saline into the AVPV. Scale bars, 20 µm. **d**, Number of TH-immunoreactive neurons in TH-expressing brain areas ($n_{\text{ablation}} = 5$, $n_{\text{control}} = 5$). Data are means + s.e.m. AVPV, anteroventral periventricular nucleus, ARC, arcuate nucleus, SN, substantia nigra, VTA, ventral tegmental area.

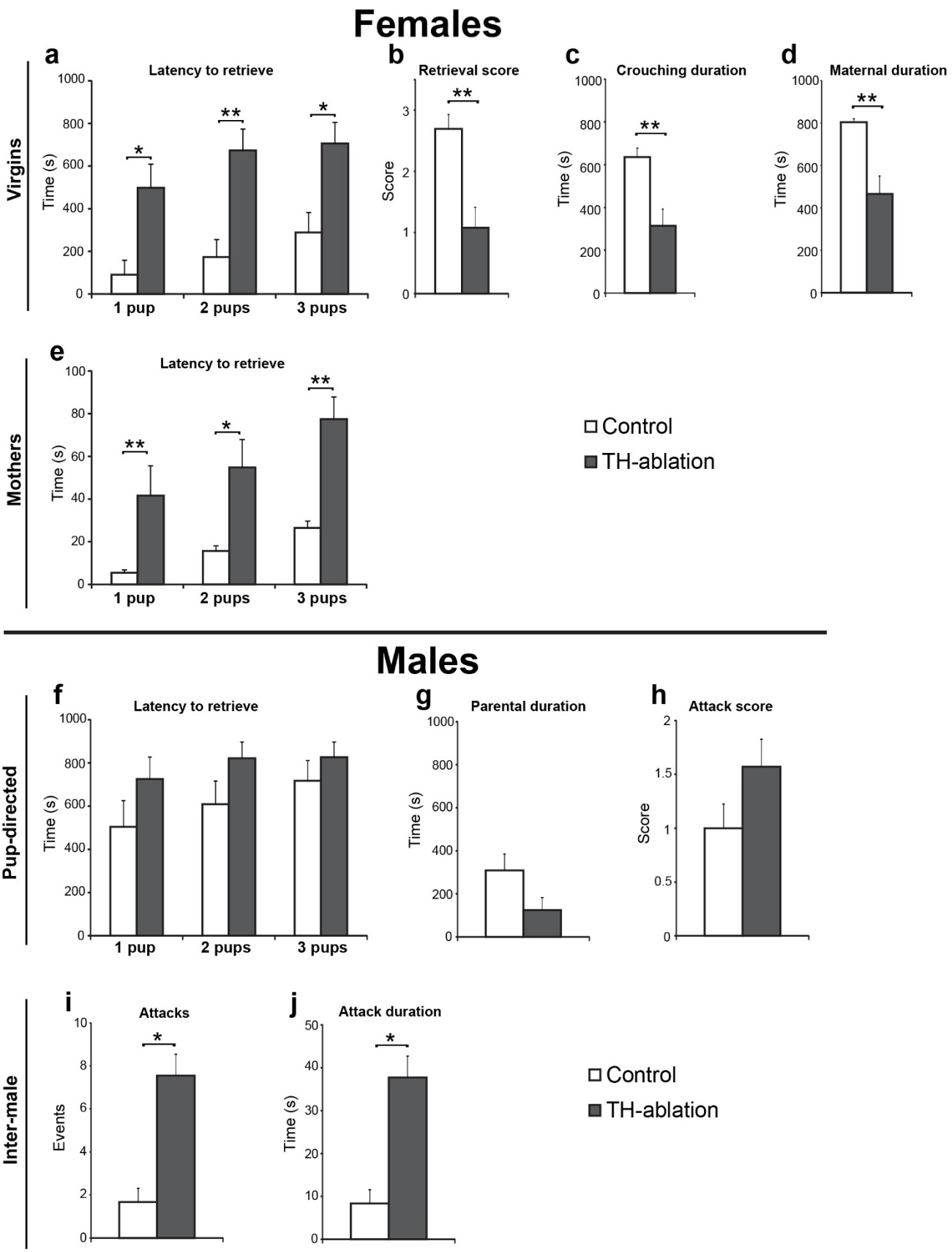

Extended Data Figure 2 | TH$^+$ ablation in AVPV impairs maternal behaviour and increases inter-male aggression. **a**–**d**, Maternal behaviour of virgin females in TH-ablation and control groups ($n_{ablation} = 13$, $n_{control} = 13$). **e**, Pup retrieval of postpartum females in TH-ablation and control groups ($n_{ablation} = 11$, $n_{control} = 11$). **f**–**h**, Pup-directed behaviours of virgin (**g**, **h**) and parental (**f**) males in TH-ablation and control groups. **i**, **j**, Inter-male aggression in TH-ablated and control groups ($n_{ablation} = 10$, $n_{control} = 10$). Data are means + s.e.m. $^*P < 0.05$; $^{**}P < 0.01$, Mann–Whitney *U*-test.

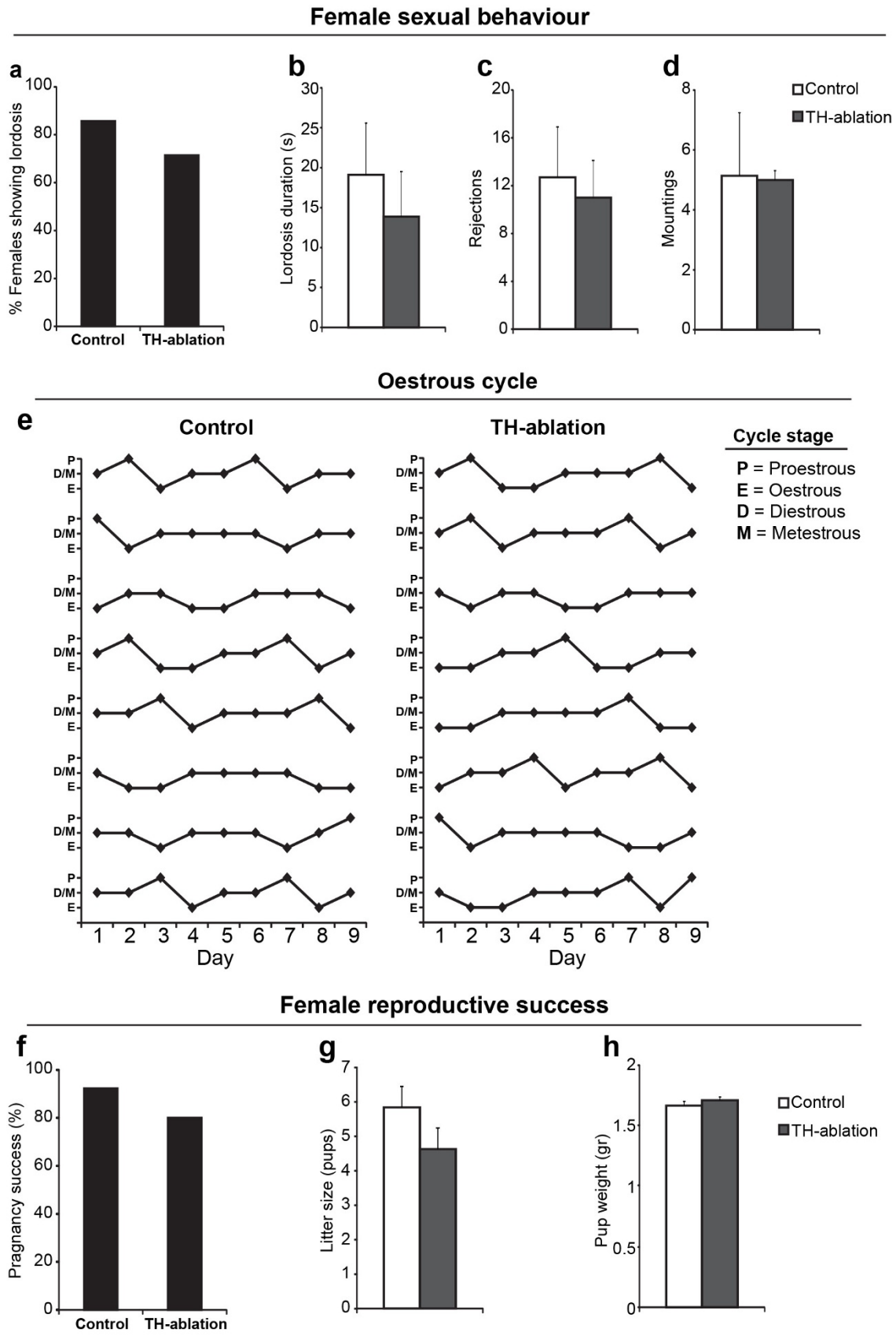

Extended Data Figure 3 | TH$^+$ ablation in female AVPV does not affect sexual behaviour and reproduction. **a**–**d**, Female sexual behaviour in TH-ablation (6-OHDA) and control (saline) groups ($n_{ablation} = 7$, $n_{control} = 7$). **a**, Percentage of females displaying lordosis behaviour. **b**, Total duration of lordosis behaviour. **c**, Number of defensive rejections of the intruder male by the subject females. **d**, Successful sexual mounting events of the intruder male on the subject females. **e**, Oestrus cycles in TH-ablation and control females ($n_{ablation} = 8$, $n_{control} = 8$). **f**–**h**, Female reproductive success in TH-ablation and control groups. **f**, Gestational success in percentage after copulation with males ($n_{ablation} = 14$, $n_{control} = 14$). Litter size (**g**) and pup weight (**h**) of TH-ablation and control females ($n_{ablation} = 12$, $n_{control} = 12$). Data are means + s.e.m.

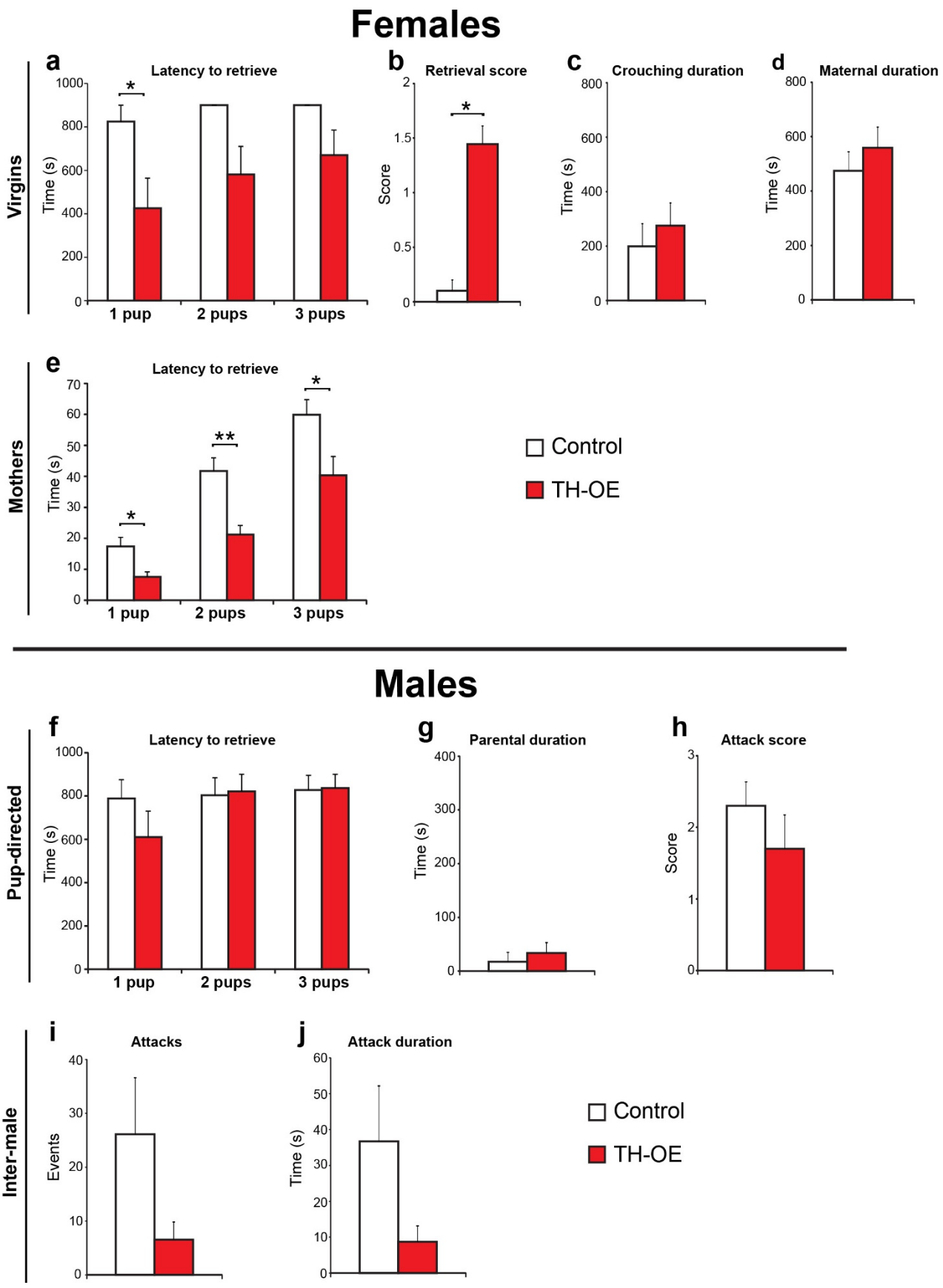

Extended Data Figure 4 | TH overexpression in TH$^+$ AVPV neurons increases maternal pup retrieval. **a**–**d**, Maternal behaviour in TH-overexpression (TH-OE) and control virgin females ($n_{OE} = 9$, $n_{control} = 10$). **e**, Pup retrieval in TH-OE and control postpartum females ($n_{OE} = 8$, $n_{control} = 7$). **f**–**h**, Pup-directed behaviours in TH-OE and control virgin (**g**, **h**) and paternal (**f**) males. **i**, **j**, Inter-male aggression in TH-OE and control males ($n_{OE} = 10$, $n_{control} = 10$). Data are mean + s.e.m. $^*P < 0.05$; $^{**}P < 0.01$, Mann–Whitney *U*-test.

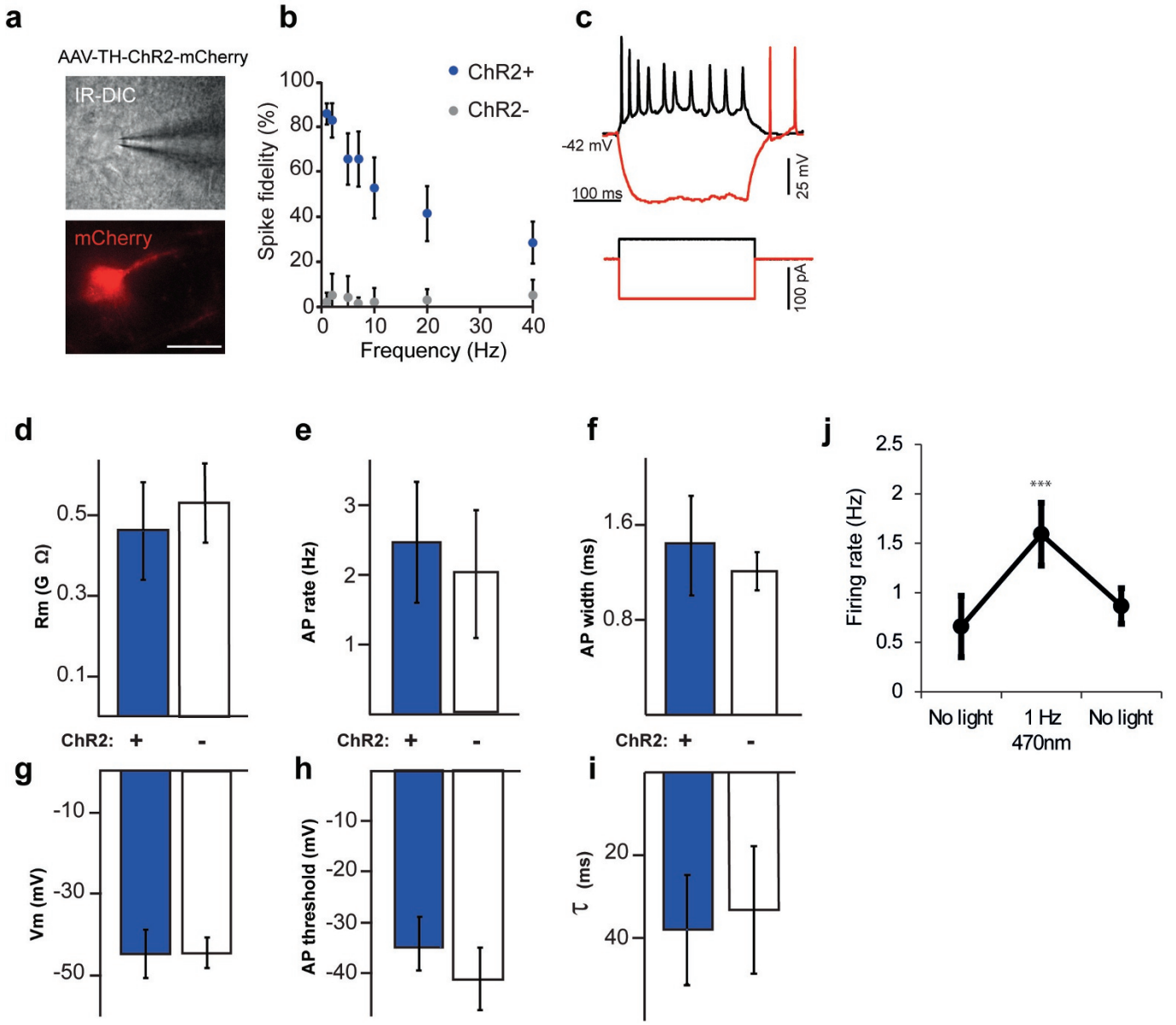

Extended Data Figure 5 | Intrinsic electrophysiological properties of TH$^+$ AVPV neurons. Whole-cell recordings were performed in acute coronal slices from TH-Cre mice co-injected with DIO-EYFP and DIO-ChR2(E123T/T159C)-mCherry viral vectors. Cells were identified based on EYFP expression and recorded in current-clamp mode. Cells were then classified as ChR2$^+$ or ChR2$^-$ based on the presence or absence of a direct, short-latency (<1 ms) light-evoked photocurrent response. **a**, Differential interference contrast (top) and mCherry fluorescence (bottom) images of a TH$^+$ AVPV cell expressing ChR2–mCherry. Scale bar, 20 µm. **b**, Light-evoked spiking fidelity in TH$^+$ AVPV neurons across varying light pulse frequencies (ChR2$^+$, $n = 12$ cells; ChR2$^-$, $n = 10$ cells). Light pulse trains containing 20 pulses (10 ms, 19 mW mm^{-2}, 475 nm) at each frequency were used to calculate response rates. Only spikes that occurred within 10 ms of light onset were calculated as direct responses. Apparent responses in ChR2$^-$ cells are attributed to the ongoing spontaneous firing of these neurons. **c**, Current clamp recording of voltage responses to negative (100 pA, red) and positive (50 pA, black) current injections in an AVPV TH$^+$ neuron. **d–i**, Intrinsic electrical properties of TH$^+$/ChR2$^+$ (blue bars) and TH$^+$/ChR2$^-$ (white bars) cells, calculated from responses to current injections as shown in **c**: input resistance (**d**), spontaneous action potential firing rate (**e**), width of action potentials at half-maximum (**f**), resting membrane potential (**g**), action potential threshold (**h**) and membrane time constant (**i**). All showed no marked difference between ChR2$^+$ and ChR2$^-$ cells (ChR2$^+$, $n = 8$; ChR2$^-$, $n = 4$). **j**, Action potential firing rates of TH$^+$/ChR2$^+$ cells recorded in whole-cell patch clamp mode before, during and after 1 Hz optogenetic stimulation (data are means ± s.e.m., ***$P < 0.05$, paired t-test, $n = 7$ cells).

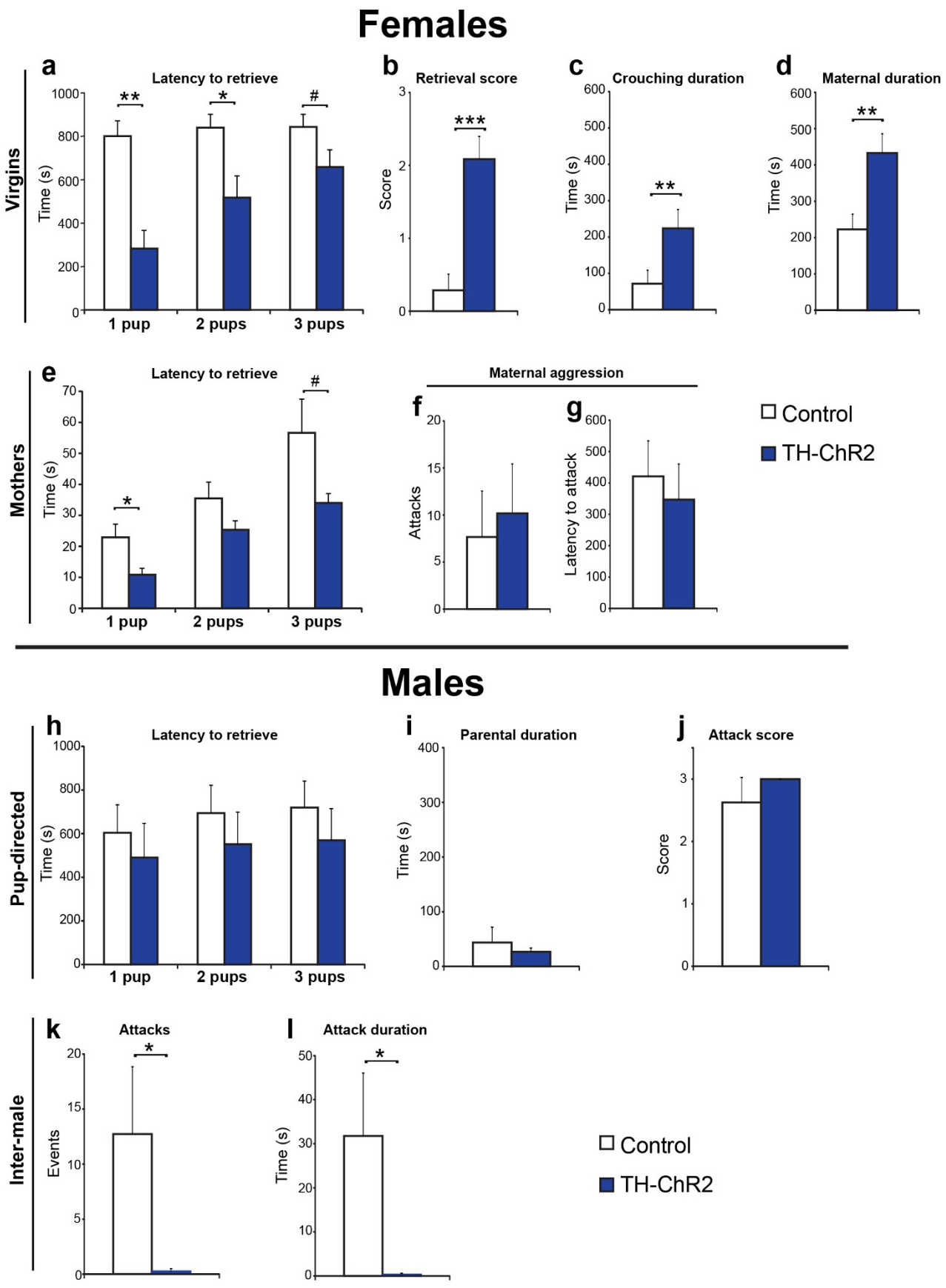

Extended Data Figure 6 | Optogenetic activation of TH$^+$ AVPV neurons increases maternal behaviour and reduces inter-male aggression. **a**–**d**, Maternal behaviour of virgin females during optogenetic activation in TH$^+$ AVPV neurons ($n_{ChR2} = 12$, $n_{control} = 14$). **e**–**g**, Pup retrieval and maternal aggression of postpartum females during optogenetic activation in TH$^+$ AVPV neurons ($n_{ChR2} = 6$, $n_{control} = 6$). **h**–**j**, Pup-directed behaviours of virgin (**i**, **j**) and paternal (**h**) males through optogenetic activation in TH$^+$ AVPV neurons. **k**, **l**, Inter-male aggression through optogenetic activation in TH$^+$ AVPV neurons ($n_{ChR2} = 10$, $n_{control} = 10$). Data are means + s.e.m. #$P = 0.09$ (**a**) or 0.05 (**e**), *$P < 0.05$; **$P < 0.01$, ***$P < 0.001$, Mann–Whitney U-test.

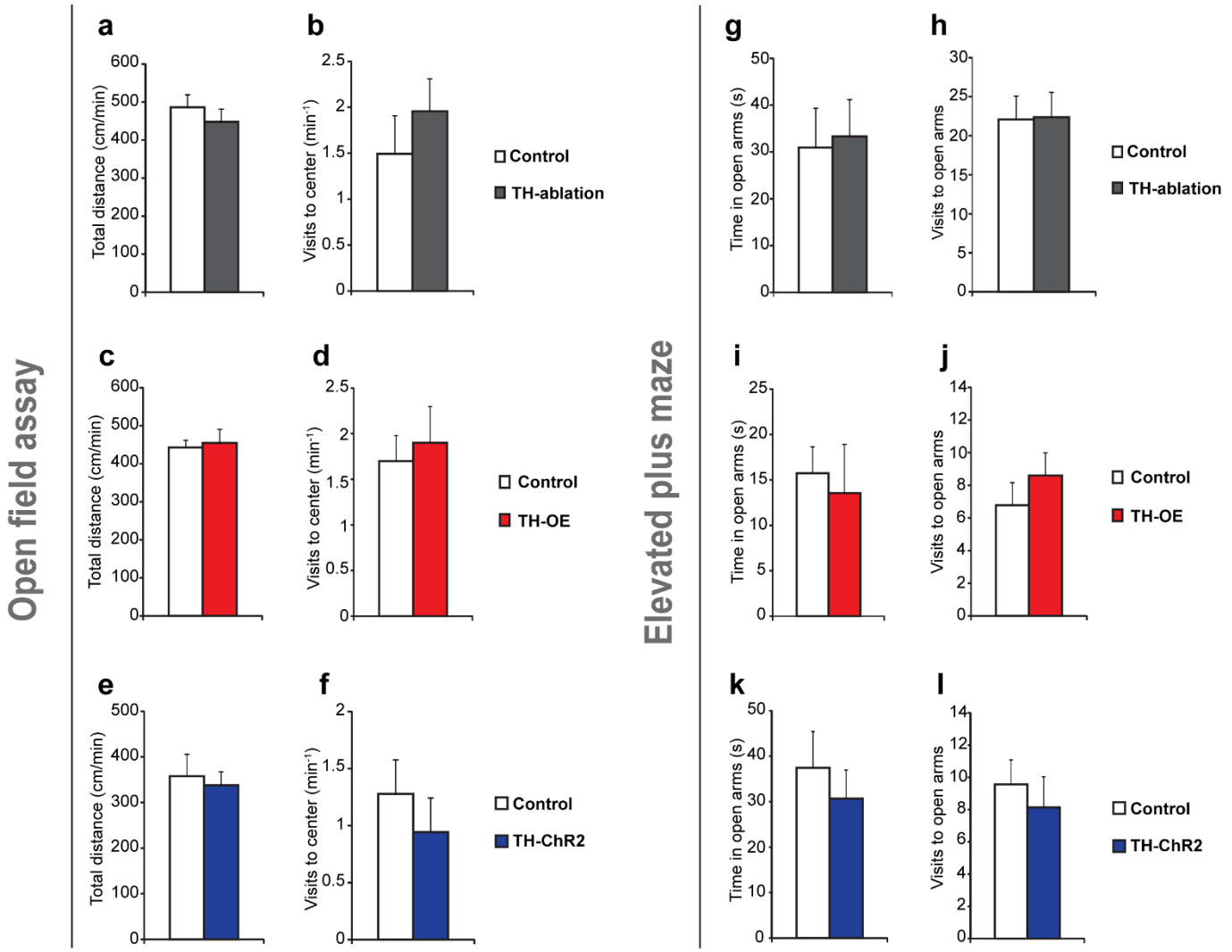

Extended Data Figure 7 | TH$^+$ AVPV neuronal manipulations do not affect locomotion or anxiety in females. **a**–**f**, Open field assay. Total distance travelled (left) and total visits to centre of the field (right) for TH-ablation (top), TH-OE (middle) and TH-ChR2 (bottom) females relative to respective control groups. **g**–**l**, Elevated plus maze assay. Total time spent in the open arms of the maze (left) and total visits to open arms (right) for TH-ablation (top), TH-OE (middle) and TH-ChR2 (bottom) females relative to respective control groups (TH-ablation, $n_{ablation} = 13$, $n_{control} = 13$; TH-OE, $n_{OE} = 10$, $n_{control} = 10$; TH-ChR2, $n_{ChR2} = 7$, $n_{control} = 9$). TH-ChR2 mice and EYFP-expressing controls were tested using attached fibre optics and blue light stimulation as described for maternal behaviour testing. Data are means + s.e.m.

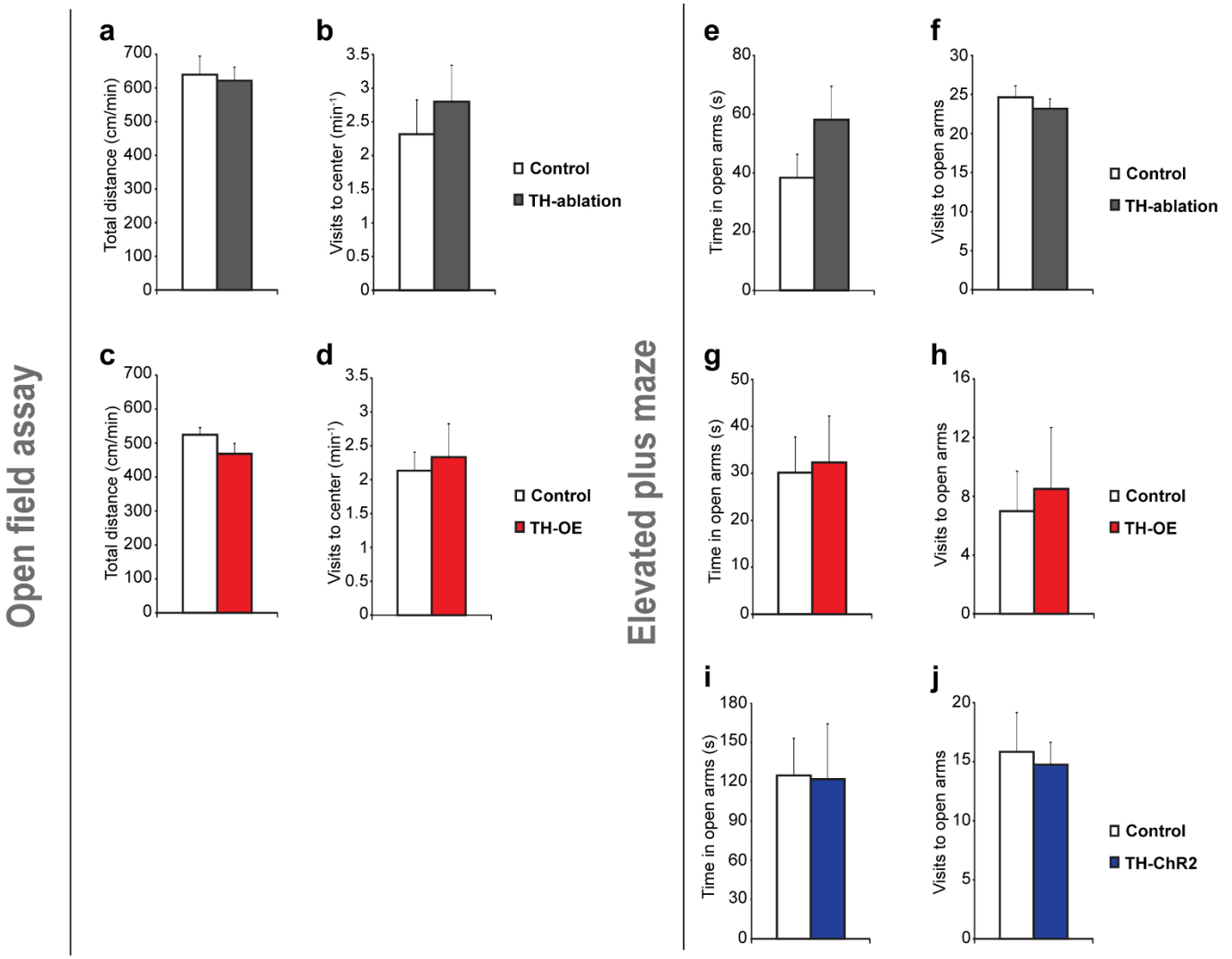

Extended Data Figure 8 | TH$^+$ AVPV neuronal manipulations do not affect locomotion or anxiety in males. **a**–**d**, Open field assay. Total distance travelled (left) and total visits to centre of the field (right) for TH-ablation (top) and TH-OE (bottom) males relative to control groups. **e**–**j**, Elevated plus maze assay. Total time spent in open arms of the maze (left) and total visits to open arms (right) for TH-ablation (top), TH-OE (middle) and ChR2 (bottom) males relative to respective control groups. (TH-ablation, $n_{ablation} = 12$, $n_{control} = 12$; TH-OE, $n_{OE} = 10$, $n_{control} = 10$; TH-ChR2, $n_{ChR2} = 4$, $n_{control} = 7$). TH-ChR2 mice and EYFP-expressing controls were tested with attached fibre optics and blue light stimulation as described for parental behaviour testing. Data are means + s.e.m.

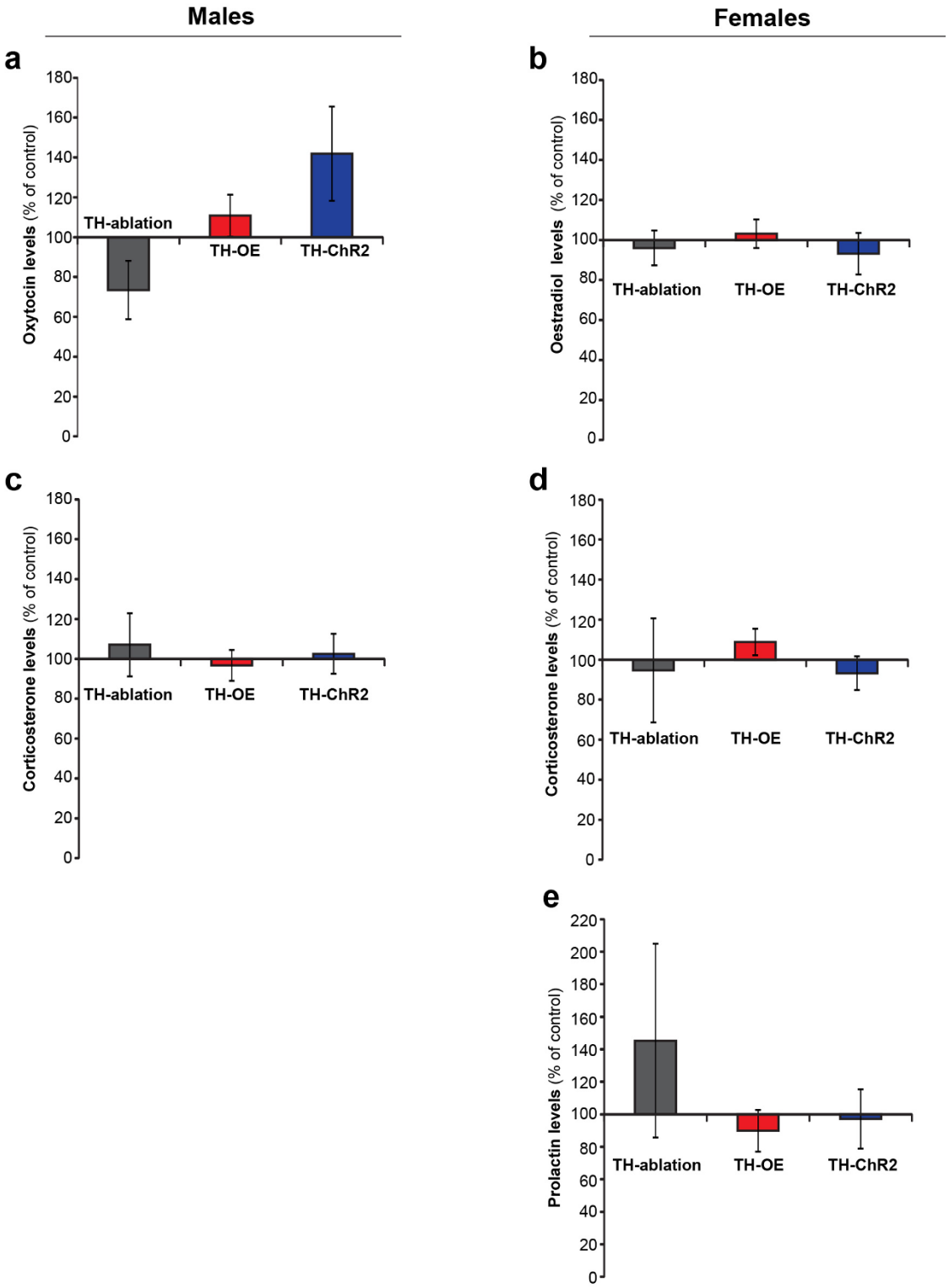

Extended Data Figure 9 | Hormones levels in plasma of TH$^+$ AVPV manipulated mice. **a**, OT levels in males (TH-ablation, $n_{ablation} = 9$, $n_{control} = 9$; TH-OE, $n_{OE} = 6$, $n_{control} = 5$; TH-ChR2, $n_{ChR2} = 7$, $n_{control} = 8$). **b**, Oestradiol levels in females (TH-ablation, $n_{ablation} = 9$, $n_{control} = 11$; TH-OE, $n_{OE} = 6$, $n_{control} = 5$; TH-ChR2, $n_{ChR2} = 10$, $n_{control} = 10$). **c**, **d**, Corticosterone levels in females (**c**) and males (**d**) (females: TH-ablation, $n_{ablation} = 6$, $n_{control} = 5$; TH-OE, $n_{OE} = 9$, $n_{control} = 9$; TH-ChR2, $n_{ChR2} = 9$, $n_{control} = 8$; males: TH-ablation, $n_{ablation} = 4$, $n_{control} = 4$; TH-OE, $n_{OE} = 8$, $n_{control} = 8$; TH-ChR2, $n_{ChR2} = 7$, $n_{control} = 7$). **e**, Prolactin levels in females (TH-ablation, $n_{ablation} = 11$, $n_{control} = 10$; TH-OE, $n_{OE} = 5$, $n_{control} = 5$; TH-ChR2, $n_{ChR2} = 6$, $n_{control} = 6$). Data are normalized to matched control groups. No significant differences were found between the TH-manipulated and control groups in the presented parameters. Data are means ± s.e.m.

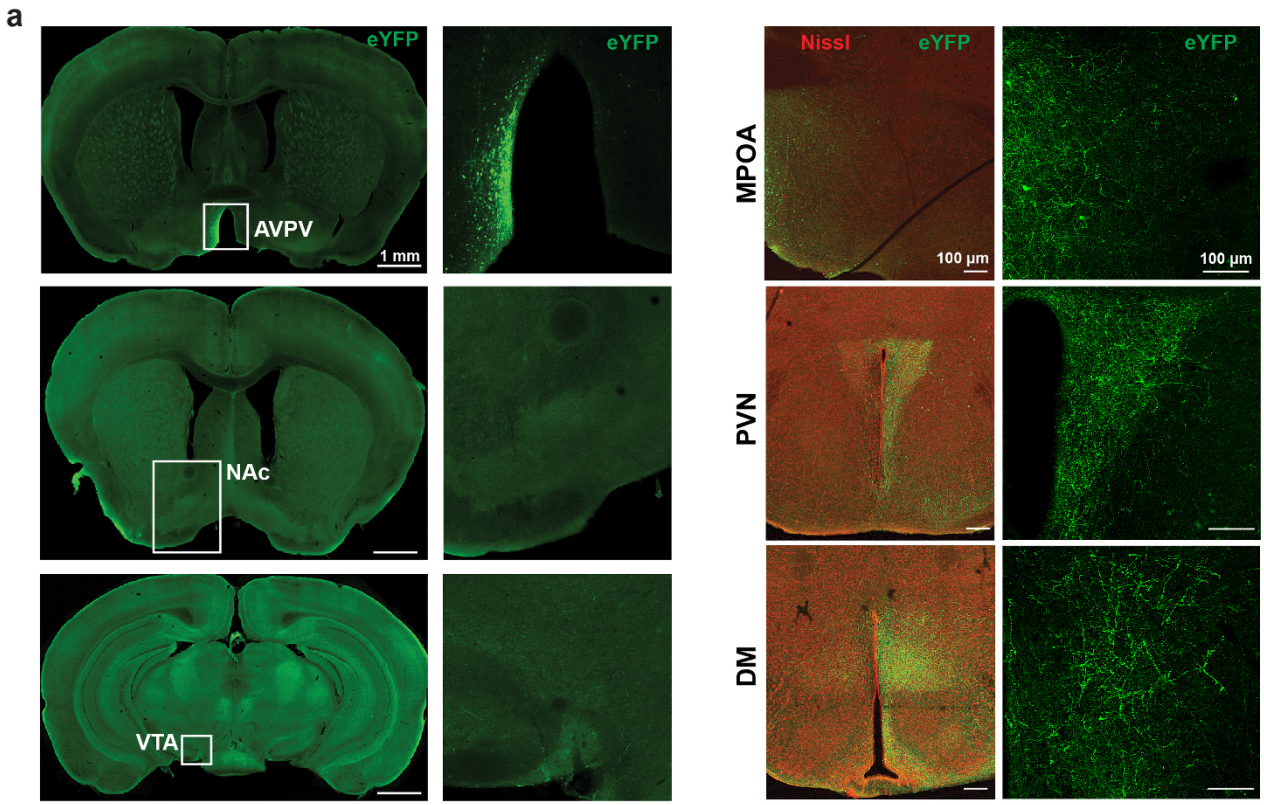

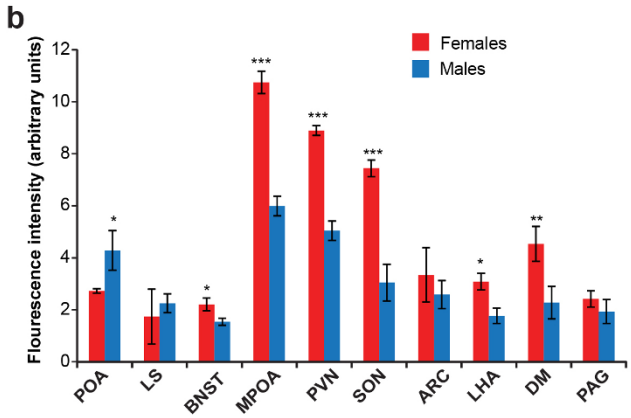

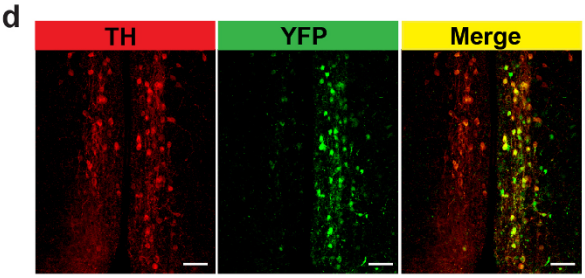

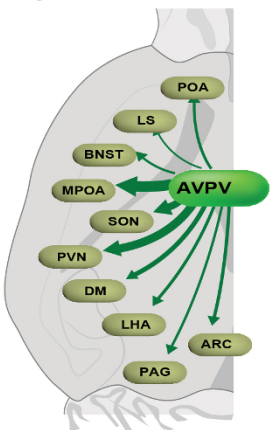

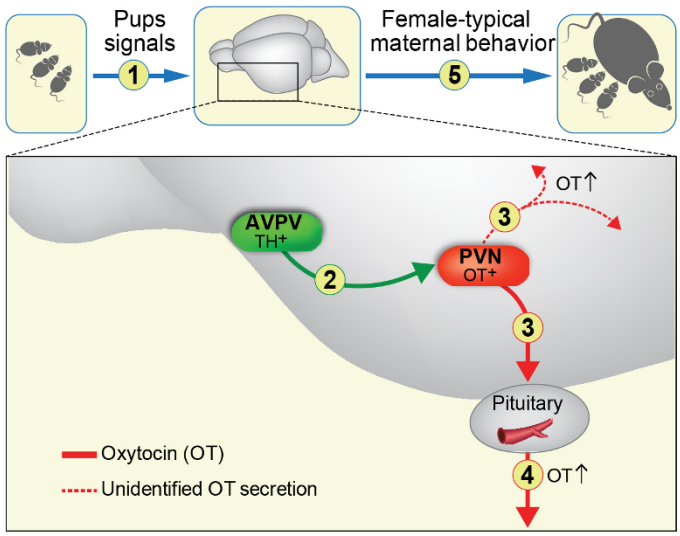

Extended Data Figure 10 | TH^+ AVPV neuronal projection and suggested model by which TH^+ AVPV neurons promote maternal care. **a**, Coronal brain sections of mice unilaterally injected with a conditional EYFP-expressing viral vector (AAV-DIO-EYFP) into the AVPV of TH-Cre female mice. Projections from TH^+ AVPV neurons into various brain structures are presented. Scale bars, 1 mm (left panel) and 100 μm (right panel). **b**, Fluorescent intensities of EYFP-labelled projection fibres of TH^+ AVPV neurons in different brain structures of TH-Cre females and males injected with a conditional EYFP-expressing viral vector (data are means ± s.e.m., females, $n = 3$; males, $n = 5$, $^*P < 0.05$, $^{**}P < 0.01$, $^{***}P < 0.001$, two-tailed Student's *t*-test). AVPV, anteroventral periventricular nucleus; POA, preoptic area; LS, lateral septum; BNST, bed nucleus of the stria terminalis; MPOA, medial preoptic area; SON, supraoptic nucleus; PVN, paraventricular nucleus; DM, dorsomedial nucleus; LHA, lateral hypothalamic area; PAG, periaqueductal grey; ARC, arcuate nucleus. **c**, Schematic illustration of projections from TH^+ AVPV neurons of adult females, in a transverse view. Arrow thickness indicates projection density, measured as fluorescent intensity of fibres labelled with EYFP. **d**, Specificity of Cre-dependent EYFP expression. Image showing a coronal section from a TH-Cre mouse injected with AAV-DIO-EYFP into the AVPV. Images show colocalization of EYFP in TH^+ neurons (green) and immunostaining for TH (red). Scale bars, 50 μm. **e**, Suggested model by which TH^+ AVPV neurons promote female-typical OT release and maternal behaviour. (1) Pup-related sensory signals induce changes in the activity of TH^+ AVPV neurons; (2) activated TH^+ AVPV neurons stimulate OT^{+} PVN neurons; (3, 4) OT^{+} PVN neurons secrete OT into central nervous system and blood; (5) maternal behaviour is facilitated.